SCIENTIFIC REPORTS

OPEN

SUBJECT AREAS:
PLASTICITY
SYNAPTIC TRANSMISSION
RECEPTORS
SENSORY SYSTEMS

Received
10 April 2012

Accepted
9 May 2012

Published
23 May 2012

Correspondence and requests for materials should be addressed to M.T. (mariomtv@hotmail.com) or G.K. (Kohr@mpimf-heidelberg.mpg.de)

Noradrenergic 'Tone' Determines Dichotomous Control of Cortical Spike-Timing-Dependent Plasticity

Humberto Salgado[2], Georg Köhr[1] & Mario Treviño[1]

[1]Department of Molecular Neurobiology, Max Planck Institute for Medical Research, Heidelberg, Germany, [2]Departamento de Neurociencias, Centro de Investigaciones Regionales ''Dr. Hideyo Noguchi'', Universidad Autónoma de Yucatán, Yucatán, México.

Norepinephrine (NE) is widely distributed throughout the brain. It modulates intrinsic currents, as well as amplitude and frequency of synaptic transmission affecting the 'signal-to-noise ratio' of sensory responses. In the visual cortex, α_1- and β-adrenergic receptors (AR) gate opposing effects on long-term plasticity of excitatory transmission. Whether and how NE recruits these plastic mechanisms is not clear. Here, we show that NE modulates glutamatergic inputs with different efficacies for α_1- and β-AR. As a consequence, the priming of synapses with different NE concentrations produces dose-dependent competing effects that determine the temporal window of spike-timing dependent plasticity (STDP). While a low NE concentration leads to long-term depression (LTD) over broad positive and negative delays, a high NE concentration results in bidirectional STDP restricted to very narrow intervals. These results indicate that the local availability of NE, released during emotional arousal, determines the compound modulatory effect and the output of STDP.

The *locus coeruleus* (LC) is a widespread projection system that supplies norepinephrine (NE) to the entire central nervous system (CNS)[1]. NE is released both tonically and phasically from axonal varicosities in the efferent circuits targeted by the LC, and directly supports arousal-related brain states and behavior[2,3]. In cortical neurons, NE has been proposed to enhance the 'signal-to-noise ratio' and to change receptive field properties by potentiating strong synaptic responses and reducing weak ones, or alternatively, by 'gating' otherwise subthreshold synaptic inputs[1].

Studies *in vitro* have shown that NE modulates intrinsic cellular excitability[4] and synaptic transmission[5,6] in the cortex. However, NE exerts complex excitatory and inhibitory effects and many contradicting results have been reported. It is possible that the distinct actions attributed to NE are in fact mediated by different effective concentrations of NE activating specific adrenergic receptor subtypes in target circuits. Indeed, the three main adrenergic receptor (AR) subtypes (α_1, α_2 and β) produce distinct synaptic actions via metabotropic G-proteins linked to different signal transduction cascades[7]. For example, in the cerebral cortex, α_1-AR and β-AR suppress and enhance evoked excitatory synaptic responses, respectively[8,9], while α_2-AR modulate inhibitory transmission[6]. In addition, AR-mediated signaling strongly controls long-term plasticity, since α_1-AR agonists selectively enable LTD and suppress LTP, while β-AR agonists enable LTP and suppress LTD[9–11]. Thus, α_1- and β-AR mediate opposing acute and long-term plastic effects. Since endogenous NE binds to all AR subtypes, the question arises as to how these opposing and mutually suppressive plastic mechanisms are evoked by NE and how they interact.

Here we show that pyramidal cells in layer II/III (LII/III PyrCs) of the mouse visual cortex are sensitive to both α_1- and β-AR agonists, and that exogenous NE produces opposing modulatory effects on excitatory transmission via these receptors when applied in the presence of the appropriate antagonists. Most importantly, these neuromodulatory effects occur with different efficacies for α_1- and β-AR. Hence, different concentrations of NE lead to strong competing modulatory interactions that determine the output of spike-timing dependent plasticity (STDP)[12]. Our results demonstrate that the plastic effects of NE are dose-dependent and receptor-specific, and provide a basis for understanding integrative functions of NE in cortical plasticity at the cellular and network level.

Results

Isolation of excitatory responses by intracellular blockade of chloride channels. In acute slices, extracellular electrical stimulation evokes overlapping excitatory and inhibitory responses in normal aCSF. Thus, to determine

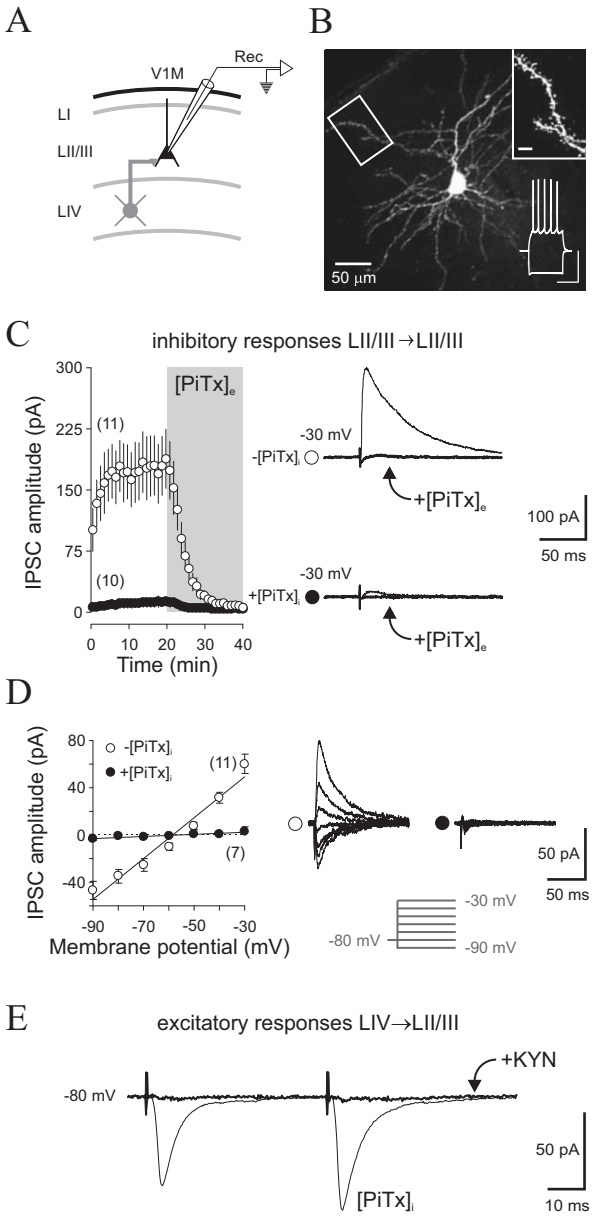

Figure 1 | Isolation of excitatory responses by intracellular chloride channel blockade. (A) Recordings were obtained from LII/III pyramidal cells (PyrCs) in the monocular portion of the primary visual cortex (V1M). (B) Sample biocytin-filled PyrC stained with streptavidin Alexa Fluor 564, and an amplified image of a dendrite with spines (upper right inset; scalebar 10 μm). A regular spiking pattern is shown in the inset lower right (scalebars: 500 ms and 50 mV). Labeled cells were not used for experiments. (C) IPSCs evoked by fixed extracellular stimulation (~100 μA) in LII/III (~100–300 μm away from the recorded cell) in the presence of GluR antagonists. Responses were acquired immediately after breaking the seal with internal solutions with or without picrotoxin (+$[PiTx]_i$, filled circles; -$[PiTx]_i$, open circles). IPSCs were eliminated by extracellular perfusion of 100 μM PiTx ($[PiTx]_e$, gray box and bold sample traces). (D) The I–V plot shows average peak IPSCs ± $[PiTx]_i$ collected ≥ 10 min after breaking the seal. Apparent GABA reversal potential (E_{GABA}) is in agreement with theoretical Cl^- equilibrium potential from the Nernst equation (in -$[PiTx]_i$: E_{GABA} = −59.5 ± 3.1 mV, n = 11). Sample traces on the right. (E) Sample LIV→LII/III synaptic currents at −80 mV in control aCSF with $[PiTx]_i$ evoked in presence (bold traces) or the absence (thin traces) of GluR antagonists; no remaining currents were observed at V_h = −30 mV (data not illustrated). Sample responses represent the average of 5 traces. Number of experiments in parentheses.

the direct effects of norepinephrine (NE) on excitatory transmission, postsynaptic inhibitory conductances must first be removed. $GABA_A$ receptors ($GABA_AR$) can be blocked by extracellular perfusion of antagonists, although this generally induces hyperexcitability and affects the entire network. To circumvent this problem, we blocked $GABA_AR$ in single recorded neurons by adding 1 mM picrotoxin to the intracellular solution (+$[PiTx]_i$)[13,14], and we assessed the efficacy of this effect in the presence of ionotropic glutamate receptor antagonists by monitoring inhibitory postsynaptic currents (IPSCs) at −30 mV (Fig. 1A, C). The blockade of $GABA_AR$ was very quick and evident just after breaking the seal, indicating rapid diffusion of $[PiTx]_i$ (Fig. 1C). Twenty minutes after breaking the seal, the IPSCs were 6.4 ± 2.9 % of those observed in control solution (-$[PiTx]_i$: 188.3 ± 36.2 pA, n = 11; +$[PiTx]_i$: 12.1± 5.4 pA, n = 10; interleaved conditions) and they were fully blocked by extracellular perfusion of 100 μM PiTx (+$[PiTx]_e$; Fig. 1C). No major changes in input resistance or resting membrane potential were observed in the presence of $[PiTx]_i$ (-$[PiTx]_i$: R_{in} = 550.2 ± 101.8 MΩ; +$[PiTx]_i$: R_{in} = 561.6 ± 139.2 MΩ; $F_{1,18}$ = 1.285, P = 0.26; -$[PiTx]_i$: RMP = −73.1 ± 1.0 mV; +$[PiTx]_i$: RMP = −72.6 ± 0.9 mV; $F_{1,18}$ = 0.079, P = 0.78; internal solution with QX-314)[15]. Thus, adding 1 mM PiTx to the internal solution blocked $GABA_AR$ channels and eliminated the evoked IPSCs at all membrane potentials tested (Fig. 1C, D), as well as the miniature IPSCs (mIPSCs)[14]. Finally, we confirmed that translaminar inhibition (i.e. LIV→LII/III; Fig. 1E) was blocked in the recording configuration used to study EPSCs, as described below.

NE exhibits different efficacies in modulating excitatory responses through alpha and beta adrenergic receptors. In cortical PyrCs, pharmacological activation of α_1- or β-adrenergic receptors (AR) depresses or potentiates synaptic excitation, respectively[8,9]. However, it remains unclear whether these two receptor subtypes are co-expressed and co-activated by NE. To improve our measurements and ensure that the effects observed are due to the exogenous NE, we first eliminated the possible influence of the endogenous NE system by disrupting the monoamine vesicular transporter with reserpine (see methods). In this condition, we investigated whether NE bidirectionally modulates EPSCs by activating α_1-AR or β-AR, incubating the slices with specific antagonists to block the contribution of either receptor: the α_1-AR was blocked with prazosin (Prz, 1 μM) and the β-AR with propranolol (Prop, 1 μM).

NE (8.75 μM) was applied to the bath solution for 20 min and the net effect was measured by averaging the EPSC amplitude over the last 10 min. In the presence of Prz, NE increased EPSC amplitude to 140.6 ± 16.2% the control levels (n = 6, P < 0.05), whereas in the presence of Prop, NE decreased the EPSC amplitude to 75.2 ± 5.7% the control levels (n = 6, P < 0.05). Both effects exhibited similar kinetics (Prz: $t_{1/2}$ = 8.7 ± 1.4 min; Prop: $t_{1/2}$ = 7.9 ± 0.8 min; P = 0.62). No changes in EPSCs (Prz+Prop: 97.9 ± 5.5%, n = 14, P = 0.42), nor in R_{in} or holding currents, were observed when the slices were treated with both antagonists (Fig. 2A), suggesting that α_2-AR do not modulate EPSCs at these synapses. Moreover, no change in the paired-pulse ratio (PPR = $EPSC_2/EPSC_1$ = 1.4 ± 0.2, n = 26) was observed after application of NE (in Prz: P = 0.88; in Prop: P = 0.69; in Prz + Prop: P = 0.50), suggesting a postsynaptic site of action. These results are consistent with the patterns of expression of AR subtypes[7,16], since α_1- and β-AR are present in LII/III cells, whereas presynaptic α_2-AR are more prominent in LI affecting inhibition[6].

We investigated the functional co-expression of α_1- and β-AR in LII/III PyrCs. Activation of β-AR with isoproterenol (Iso, 10 μM, 10 min) increased EPSC amplitude to 119.9 ± 6.1% (n = 9, P < 0.05) the control levels, while subsequent activation of α_1-AR with methoxamine (Mtx, 5 μM, 10 min) decreased the amplitude to 76.1 ± 4.4% (P < 0.05; **Fig 2B**). Perfusion of the agonists did not affect the

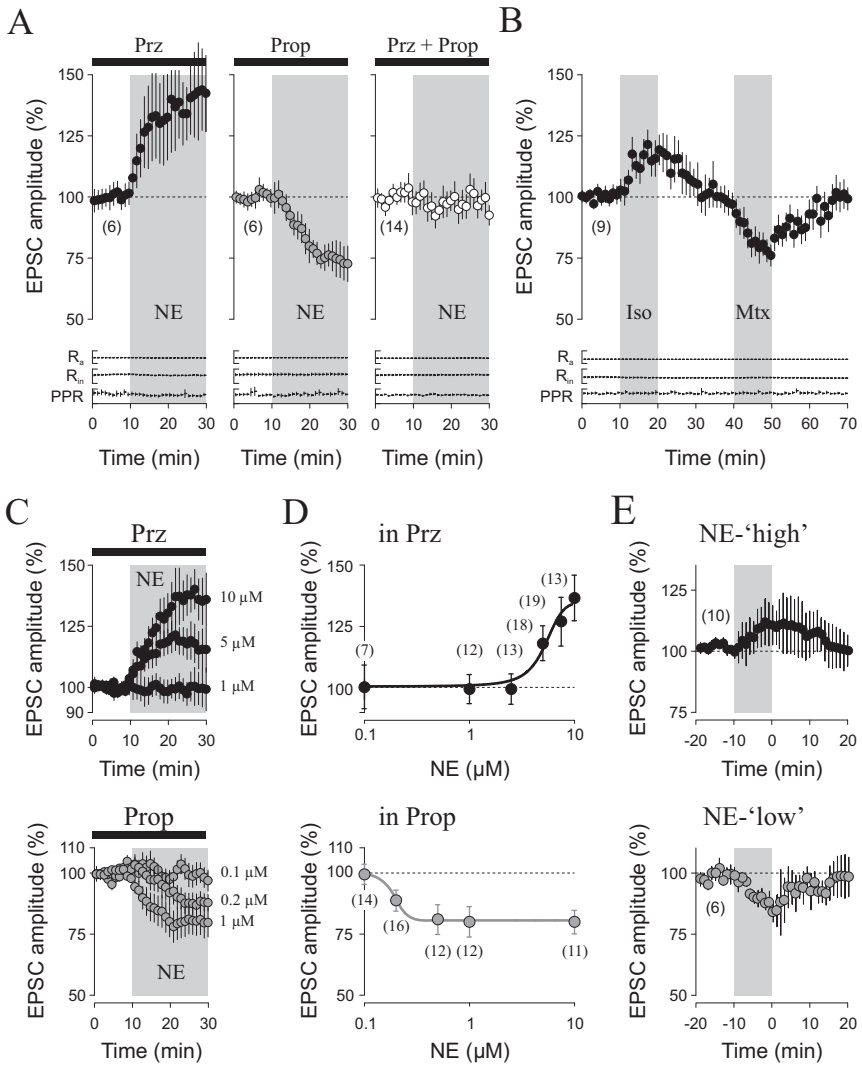

Figure 2 | Norepinephrine modulates excitatory responses via α_1- and β-ARs. (A) Norepinephrine ($[NE]_{high}$ = 8.75 µM NE) potentiated EPSCs in prazosin (Prz, 1 µM) and decreased EPSCs in propranolol (Prop, 1 µM), yet it had no effect in Prz + Prop (no change in holding current; data not illustrated). Similar kinetics for both effects. No change in R_a, R_{in} or PPR were detected (scalebars: 20 MΩ, 200 MΩ, 2). (B) EPSCs amplitude augmented with isoproterenol (Iso, 10 µM, 10 min) and after washout, it decreased with methoxamine (Mtx, 5 µM, 10 min). Both effects were reversible. (C,D) NE-concentration-response curves for EPSCs in the presence of prazosin (Prz, upper panels) or propranolol (Prop, lower panels). The ordinate in (D) indicates the change in EPSC amplitude averaged over the last 10 min of NE application. Lines are generalized logistic functions. (E) Reversible effects of $[NE]_{high}$ and $[NE]_{low}$ (0.33 µM NE) in control aCSF. Number of experiments in parentheses.

PPR and the effects were fully reversed within 20 min of washing out the specific agonists (Iso, P = 0.23; Mtx, P = 0.69). These findings indicate that PyrCs from the visual cortex co-express α_1- and β-AR, which modulate EPSCs in opposite directions.

We next characterized the dose-response curves of NE following blockade of α_1-AR or β-AR. In the presence of Prz, bath-application of NE produced a dose-dependent enhancement of EPSC amplitude (NE 0.1 µM: 100.4 ± 8.8%, n = 13, P = 0.86; 1 µM: 99.4 ± 6.0%, n = 12, P = 0.73; 2.5 µM: 99.4 ± 6.2%, n = 13, P = 0.75; 5 µM: 118.1 ± 7.1%, n = 18, P < 0.05; 7.5 µM: 126.9 ± 10.0%, n = 19, P < 0.05; 10 µM: 136.6 ± 9.3%, n = 13, P < 0.05; **Fig 2C, D** upper panels). By contrast, in the presence of Prop, NE produced a dose-dependent reduction in EPSC amplitude (in Prop, NE 0.1 µM: 99.2 ± 4.2%, n = 14, P = 0.48; 0.2 µM: 88.6 ± 4.2%, n = 16, P < 0.05; 0.5 µM: 80.8 ± 6.0%, n = 12, P < 0.05; 1 µM: 79.9 ± 6.2%, n = 12, P < 0.05; 10 µM: 79.8 ± 4.7%, n = 11, P < 0.05; Fig. 2C, **D** lower panels). We fitted generalized logistic functions to the data points (Fig. 2D) and found that the half maximal effective NE concentrations under α_1-AR or β-AR blockade differed more than 20-fold ($EC_{50,Prz}$ = 5.21 µM NE; $EC_{50,Prop}$ = 0.19 µM NE). Likewise, the concentrations required to reach 99% of the maximal effects were 8.75 µM NE (hereafter referred to as '$[NE]_{high}$') in the presence of Prz, and of 0.33 µM NE ('$[NE]_{low}$') in the presence of Prop. Thus, saturated neuromodulatory actions of NE already occur at concentrations below 10 µM. In aCSF and in the absence of AR antagonists, bath applied $[NE]_{low}$ (10 min) decreased the EPSC amplitude to 84.0 ± 5.8% (n = 6, P = 0.03) the control levels, while $[NE]_{high}$ increased EPSCs to 112.2 ± 4.2% (n = 10, P = 0.01; Fig. 2E). In both cases, the changes were reversed 20 min after NE washout ($[NE]_{high}$, P = 0.63; $[NE]_{low}$, P = 0.39). Notably, the maximal acute effects of $[NE]_{low}$ and $[NE]_{high}$ in aCSF were smaller than those observed in the presence of the antagonist (in Prop, NE 8.75 µM: 132.5 ± 17.5%, at 10 min; Fig. 2A), suggesting that $[NE]_{low}$ activates mainly α_1-AR while $[NE]_{high}$ co-activates α_1-AR and β-AR, triggering competing effects.

The NE concentration determines the compound modulation of spike-timing-dependent plasticity in the mouse visual cortex. Neuromodulatory receptors have been implicated in modulating

the efficacy of spike-timing-dependent plasticity (STDP) in brain slices[17]. One would expect that the plastic effect of a single neuromodulator receptor subtype should increase with agonist concentration. But, does NE leads to interactions between the plastic effects of α_1- and β-AR affecting the outcome of STDP? We investigated whether the different concentrations of NE, $[NE]_{high}$ and $[NE]_{low}$ influenced STDP plasticity. After recording at least 10 min of baseline EPSCs, NE was applied for 10 min and the STDP-protocol was delivered at the end of the drug application (see methods). In control aCSF, although inhibition was blocked intracellularly, we observed no lasting changes in EPSCs when the postsynaptic burst preceded presynaptic activation (negative delay of $\Delta t = -10.4 \pm 0.5$ ms: 103.1 ± 6.4%, n = 13, $P = 0.11$; Fig. 3A, empty circles) or *vice versa* (positive delay of $\Delta t = +7.1 \pm 0.2$ ms: 102.7 ± 6.6%, n = 11, P = 0.13; Fig. 3B empty circles), consistent with previous observations[18]. However, priming synapses with $[NE]_{high}$ led to timing-dependent long-term depression (t-LTD) for pairings with a negative delay (NE 8.75 μM at $\Delta t = -9.8 \pm 0.2$ ms: 70.5 ± 6.8%, n = 7, P < 0.05; Fig. 3A, black circles) and long-term potentiation (t-LTP) for a positive delay (NE 8.75 μM at $\Delta t = 6.5 \pm 0.3$ ms: 126.6 ± 4.6%, n = 11, P < 0.05; Fig. 3B, black circles). Notably, larger negative or positive intervals produced no persistent changes with $[NE]_{high}$ (NE 8.75 μM at $\Delta t = -19.1 \pm 0.6$ ms: 96.9 ± 7.6%, n = 9, P = 0.63; $\Delta t = 17.4 \pm 0.4$ ms: 105.5 ± 4.4%, n = 8, P = 0.15; Fig. 3C, D, black circles). By contrast, when pairings were combined with $[NE]_{low}$, t-LTD was observed both at negative and positive delays (NE 0.33 μM at $\Delta t = -18.75 \pm 0.6$ ms: 74.3 ± 5.4%, n = 8, P < 0.05; $\Delta t = -9.4 \pm 0.4$ ms: 70.5 ± 12.0%, n = 8, P < 0.05; $\Delta t = 6.4 \pm 0.5$ ms: 71.9 ± 4.3%, n = 8, P < 0.05; $\Delta t = 16.5 \pm 0.4$ ms: 81.2 ± 5.1%, n = 11, P < 0.05; Fig. 3A–D, grey circles). This indicates that NE concentration determines the output of STDP.

Neither application of NE nor induction of associative plasticity affected the average PPR or R_{in} (**Fig 3A, B**) and no lasting changes were induced when NE was applied in conjunction with either pre-synaptic activation alone (NE 8.75 μM: 99.2 ± 5.4%, n = 10, paired t-test, P = 0.63; NE 0.33 μM: 101.8 ± 6.3%, n = 6, P = 0.39; data not illustrated) or with postsynaptic firing alone (NE 8.75 μM: 98.4 ± 3.6%, n = 10, P = 0.84; NE 0.33 μM: 95.8 ± 2.8%, n = 10, P = 0.11; data not illustrated). Interestingly, we could not induce STDP when priming was attempted with single postsynaptic spikes instead of bursts (NE 8.75 μM at $\Delta t = 7.4 \pm 0.5$ ms: 94.2 ± 8.2%, n = 6, P = 0.45; data not illustrated). Thus, in our recording conditions, NE permitted the induction of STDP only when pre-synaptic and robust postsynaptic activity were combined.

We explored the priming effects of NE on STDP also at several larger delays (Fig. 3E, F). We found that $[NE]_{low}$ enabled t-LTD over a wide range of negative ($\Delta t \geq -20$ ms) and positive ($\Delta t \leq +50$ ms) delays (Fig. 3E), whereas $[NE]_{high}$ enabled t-LTD only at a short negative delay ($\Delta t = -9.8 \pm 0.2$ ms) and t-LTP for a short positive delay ($\Delta t = +6.5 \pm 0.3$ ms; Fig. 3F). We conclude that the output of

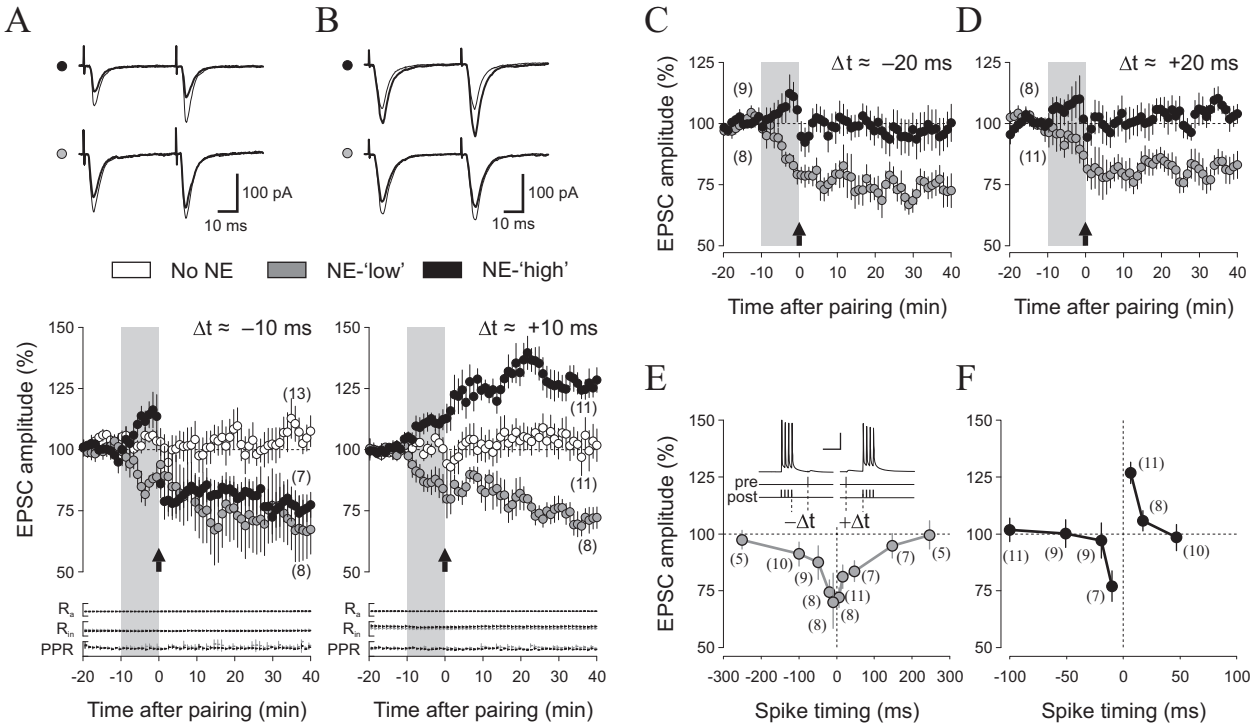

Figure 3 | Norepinephrine concentration determines the STDP timing window. (A–D) Pairings at −10 ms or +10 ms without NE (open circles, A and B) induced no lasting changes in EPSCs. Bath application of $[NE]_{high}$ (NE, 8.75 μM, black filled circles) increased EPSCs and allowed the expression of LTD with pairings at −10 ms (A) and LTP at +10 ms (B), whereas no plastic changes were detected at ± 20 ms (C–D). Perfusion of $[NE]_{low}$ (NE, 0.33 μM, gray filled circles) reduced EPSCs and enabled the expression of LTD at ± 10 ms and ± 20 ms (A–D). Sample traces before (thin lines) and 40 min after (thick lines) the STDP protocol are shown above the panels A and B. The STDP protocols are depicted by black arrows and were delivered at t = 0 min (duration is not represented in the time axis). No changes in R_a, R_{in} or PPR were detected (scalebars: 20 MΩ, 200 MΩ, 2). (E–F) Spike-timing windows for STDP induced by priming synapses with $[NE]_{low}$ (gray circles, E) or $[NE]_{high}$ (black circles, F). The changes in EPSC amplitude (as a percentage of control), calculated as an average over 30–40 min after conditioning, are plotted against the spike timing delays used during induction. Assuming that the data can be approximated by exponential functions[19,22]: ($A^+\exp(t/\tau^+)$ for $\Delta t < 0$ and $A^-\exp(t/\tau^-)$ for $\Delta t \geq 0$): in NE 0.33 μM: $A^- = -33.3\%$, $\tau^- = 64.7$ ms, n = 40, $A^+ = -31.3\%$, $\tau^+ = 40.7$ ms, n = 38; in NE 8.75 μM: $A^- = -62.4\%$, $\tau^- = 4.9$ ms, n = 36, $A^+ = +47.5\%$, $\tau^+ = 9.7$ ms, n = 29). The upper panel in E shows sample traces of pairing paradigms with negative (left) and positive (right) timing delays. Scalebars represent 50 mV (vertical) and 50 ms (horizontal). All recordings in normal aCSF. Number of experiments in parentheses.

STDP is not rigid, as $[NE]_{low}$ was associated with a broad t-LTD-only STDP-window, while $[NE]_{high}$ led to bidirectional STDP, restricted to very narrow time intervals. Through a dichotomous action by activating α_1- and β-AR, the noradrenergic 'tone' increased the temporal contrast of STDP.

NE mediates competing modulation of t-LTP and t-LTD. Our results suggest that NE generates a compound neuromodulatory effect that determines the outcome of STDP. The question arises as to whether NE induces opposing long-term neuromodulatory effects through α_1-AR and β-AR. We reasoned that if compound plastic effects by NE are mediated by co-activation of these two receptors, then pharmacological blockade of one receptor subtype should unmask the plastic effects mediated by NE acting on the competing receptor.

Accordingly, in the presence of the α_1-AR blocker prazosin, $[NE]_{high}$ led to t-LTP with STDP pairings at a negative delay (Prz + NE 8.75 μM at $\Delta t = -11.36 \pm 0.3$ ms: 120.5 ± 8.3%, n = 11, $P < 0.05$; NE 8.75 μM at $\Delta t = -9.8 \pm 0.2$ ms: 70.5 ± 6.8%, n = 7, $P < 0.05$; Fig. 4A), while in the presence of the β-AR blocker propranolol, $[NE]_{high}$ led to t-LTD at a positive delay (Prop + NE 8.75 μM at $\Delta t = 7.9 \pm 1.0$ ms: 80.4 ± 6.4%, n = 11, $P < 0.05$; NE 8.75 μM at $\Delta t = 6.5 \pm 0.3$ ms: 126.6 ± 4.6%, n = 11, $P < 0.05$; Fig. 4B). Thus, the gating of STDP by NE depends upon competing processes that are mediated by α_1-AR and β-AR, which control LTD and LTP, respectively.

Discussion

We have investigated the role of NE in the acute and long-term modulation of excitatory transmission in LII/III PyrCs from the mouse visual cortex. The rate of AR activation depends on the concentration of NE and its affinity for these receptors, which differs for α_1- and β-AR[7]. Using increasing concentrations of NE in the presence of α_1- or β-AR antagonists, we determined the EC_{50} values for the modulation of EPSCs by NE acting through α_1- and β-AR in LII/III PyrCs. Remarkably, these values differed more than 20-fold. Opposing NE modulation of EPSCs was mediated by α_1- and β-AR, and it was abolished in the presence of antagonists for both receptors. Hence, the neuromodulatory actions of NE on these synapses appear to be predominantly mediated through α_1- and β-AR, and not through α_2-AR. Furthermore, LII/III PyrCs were co-sensitive to sequential application of selective α_1- and β-AR agonists, demonstrating the co-expression of these receptors in the recorded cells. Acute modulation of EPSCs was fully reversible and did not affect paired-pulse ratios, in contrast to what is observed for IPSCs[6]. Unlike the arbitrary ratios of AR activation achieved with specific agonists, the use of NE enables a specific profile of activation of α_1- and β-AR. Based on the EC_{50} values, we selected two NE concentrations: one that targeted α_1-AR ($[NE]_{low}$) and depressed EPSCs and one that co-activated α_1- and β-AR ($[NE]_{high}$). Co-activation was reflected as a reduced EPSC potentiation by $[NE]_{high}$ compared to that obtained in the presence of the α_1-AR antagonist prazosin.

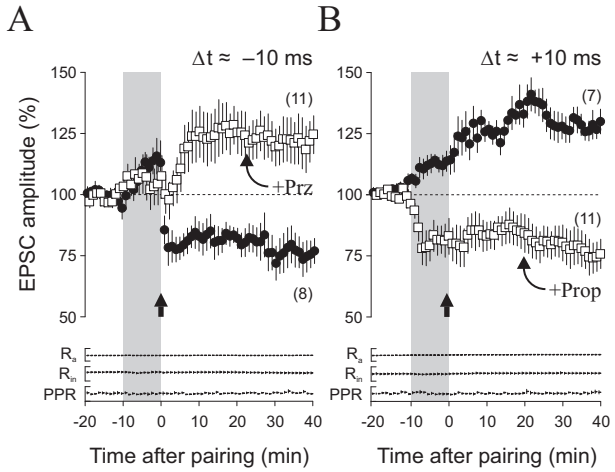

Figure 4 | Norepinephrine exerts competing modulatory actions for STDP. In normal aCSF, pairings at −10 ms with $[NE]_{high}$ led to LTD (black circles, A) while pairings at +10 ms led to LTP (black circles, B) (same data as in Fig. 3). If slices were incubated in prazosin (+Prz), pairings at −10 ms led to LTP (white squares, A), whereas in propranolol (+Prop), pairings at +10 ms lead to LTD (white squares, B). No significant changes in R_a, R_{in} or PPR (scalebars: 20 MΩ, 200 MΩ, 2). Similar modulatory actions to those observed in cells from Fig. 2A (repeated measures two-factor ANOVA, $[NE]_{high}$ in Prop: $F_{1,153} = 0.2$, $P = 0.65$; $[NE]_{high}$ in Prz: $F_{1,180} = 3.5$, $P = 0.08$). Delivery of the STDP protocol is depicted by black arrows. Number of experiments in parentheses.

The temporal windows for STDP produced with $[NE]_{low}$ and $[NE]_{high}$ are in contrast with 'canonical' STDP which is temporally asymmetric and has a broader region for t-LTD than for t-LTP[19–21]. The symmetry (and anti-symmetry) observed in our STDP windows may reflect the isolation from the effects of endogenous catecholamines, although it may also depend on other factors[12]. The broadened t-LTD window that we observed with $[NE]_{low}$ favors a generalized build-up of synaptic depression and could contribute to the stabilization of postsynaptic firing rates under conditions of excessive excitatory drive[22].

We have shown that pharmacological activation of α_1-ARs primes visual cortical neurons to produce a form of visual experience-induced LTD *in vivo*[10], with relevant behavioral consequences[23]. This form of α_1-AR LTD is expressed at ascending excitatory inputs carrying visual information to layer II/III and correlates with a selective and orientation-specific decrease in visual discrimination performance of sinusoidal drifting gratings at high spatial frequencies. Thus, at least a fraction of ARs participates in allowing visual

information to produce cortical plasticity in a stimulus-specific manner[23]. Our results here suggest that low levels of endogenous NE could mediate such a form of α_1-AR LTD, whereas a higher NE 'tone' could enable LTP with positively correlated activity, a likely scenario during sensory processing *in vivo*. Concomitant changes in and into local inhibition cannot be discarded[6,24].

Differences in LC activity may affect the NE concentrations released diffusely in downstream nuclei. The firing rates of LC neurons vary with periods of wakefulness and arousal, and they are virtually silent during rapid eye movement (REM) sleep[3]. During wakefulness, specific modes of LC firing can be distinguished, and are thought to participate in optimizing reward-seeking behavior[1–3,7]. It is tempting to speculate that the 'tones' of NE during wakefulness and sleep participate in reorganizing cortical synaptic weights in a spike-timing dependent manner. The higher NE levels present during wakefulness and non-REM stages could promote bidirectional plasticity of active sensory inputs, while the lower NE levels found during REM sleep may favor the generalized build-up of synaptic depression of active synapses. Action potential driven quantal release of NE from central neurons occurs by exocytosis of vesicles with intravesicular concentration of ~0.4–1 M NE[25] which might well support conditions with synaptic NE concentrations in the micromolar range (i.e. such as NE-'high'). Moreover, a mechanism for gating generalized LTD during sleep is attractive, as it could contribute to increase in the 'signal-to-noise ratio' of relevant memories, remove spurious associations[26] and contribute to synaptic homeostasis[27,28]. In contrast, the higher NE levels during emotional arousal could facilitate the formation of new memories[29]. The present results contribute to our understanding of how NE interacts with divergent AR signaling cascades to support generalized weakening and restrictive strengthening of cortical synapses.

Methods

Animals. A total of 133 wild-type male C57BL/6 mice (Charles River; Sulzfeld, Germany) were used in the present study. Mice were housed in groups of up to 10 per cage (type III, 825 cm^2; Ehret, Emmendingen, Germany) with *ad libitum* access to food and water. To study slice preparations in the absence of endogenous NE, catecholamine pools were depleted by disrupting the monoamine vesicular transporter with reserpine (5 mg/kg; in 10% 1,2 propanediol + 50 µl glacial acetic acid; Fluka), administered i.p. at 8:00 p.m. Mice displayed pronounced catalepsy and minimal locomotor activity 12–16 h later, at which point slices were prepared. All experiments were conducted at the Max Planck Institute for Medical Research in accordance to the animal welfare guidelines of the Max Planck Society and were approved by the regional commission in Karlsruhe (G-171/10).

Electrophysiological experiments. Coronal slices of the visual cortex (350 µm) from postnatal day (P)26 ± 2 mice (average weight, 13 ± 2 g) were cut in dissection buffer at 4°C containing (in mM): 220 sucrose, 3.5 KCl, 1.25 NaH_2PO_4, 3 $MgCl_2$, 1 $CaCl_2$, 25 $NaHCO_3$ and 10 dextrose. Individual slices were gently stored in normal artificial cerebrospinal fluid (aCSF) for at least 1.5 hrs before recording. Normal aCSF was similar to the dissection buffer except that the sucrose was replaced by 124 mM NaCl, $MgCl_2$ was lowered to 1.5 mM, and the $CaCl_2$ was raised to 2.5 mM. Both the dissection buffer and normal aCSF were saturated with 95% O_2/5% CO_2 (pH 7.4). The slices were transferred to a submerged recording chamber and perfused with aCSF (2 ml/min at 30°C). Whole-cell recordings (IR-DIC, Axioskop 2 FS, Carl Zeiss AG, Göttingen, Germany) were obtained from regular spiking pyramidal-shaped cells from LII/III located in the monocular portion of the visual cortex (V1M, ~1.5–2 mm lateral of lambda, ~35% depth from the Pia), as described previously[23]. Borosilicate recording pipettes (2–4 MΩ) were filled with intracellular solution containing (in mM): 130 (K)Gluconate, 10 KCl, 0.2 EGTA (pH = 8), 10 HEPES, 4 (Mg)ATP, 0.5 (Na_3)GTP and 10 (Na_2)Phosphocreatine (pH = 7.25, 280–290 mOsm). To isolate postsynaptic glutamatergic responses, picrotoxin was added to the intracellular solution (1 mM $[PiTx]_i$[13,14]. To record inhibitory postsynaptic currents (IPSCs) at different membrane potentials, 5 mM QX-314 (lidocaine N-ethyl bromide) and a cocktail of glutamate antagonists (2.5 mM kynurenic acid + 10 µM DNQX) were added to the intra- and extracellular solutions, respectively. Only cells with holding currents ≤ 100 pA at V_h = −80 mV, series resistance ≤ 20 MΩ and input resistance ≤ 200 MΩ were studied (Fig. 1E, 2–4; internal solution without QX-314). Cells were discarded if any of these parameters changed by ≥ 20% during the course of the experiment (−10 mV, 100 ms). Electrophysiological data were filtered at 2 kHz and digitized at 10 kHz using an EPC-10/Patchmaster amplifier (Heka Elektronik, Lambrecht, Germany).

Electrical stimulation and induction of plasticity. Excitatory synaptic responses in LII/III were evoked with paired pulses (inter-stimulus interval = 50 ms) at 0.05 Hz through an extracellular monopolar stimulating electrode (125 mM NaCl; 0.2 ms, ≤ 150 µA) placed in LIV (~300 µm vertically below the recorded neuron). The stimulus intensity was adjusted to evoke small (≤ 200 pA), simple-waveform, short onset latency (≤ 2 ms) monosynaptic excitatory postsynaptic currents (EPSCs[20]), and the paired-pulse ratio was calculated as PPR = $EPSC_2/EPSC_1$. To induce spike-timing dependent plasticity (STDP), the recording mode was switched from voltage-clamp to current-clamp. The protocol consisted of pairing presynaptic stimulation with a single action potential or a burst of four postsynaptic action potentials evoked by passing suprathreshold depolarizing current steps through the recording pipette (1.5–2.5 nA, 1 ms at 100 Hz). Associative pairing consisted of 200 pairing epochs (one burst paired with stimulation of the test pathway at different delays) delivered at 1 Hz. The strength of the EPSCs was measured as the peak amplitude response recorded at V_h = −80 mV. Changes in synaptic strength were quantified as changes in the EPSCs amplitude normalized with respect to the mean baseline response obtained during the first 10 minutes of stable recording before drug application. Acute changes were calculated as the average EPSC amplitude measured over 10–20 min during drug application and the magnitude of plasticity was taken as the average EPSC amplitude recorded over 30–40 min after the conditioning stimulus. Pairings were performed at the end of agonist application. To prevent oxidation, norepinephrine stocks were prepared freshly in aCSF containing sodium ascorbate (40 µM).

Statistical Analysis. Statistical comparisons were performed using paired Student's t tests (to analyze changes in synaptic responses) and ANOVA (to compare groups formed by individual neurons). The significance level was set at $P < 0.05$. All results are shown as averages ± SEM.

1. Berridge, C. W. & Waterhouse, B. D. The locus coeruleus-noradrenergic system: modulation of behavioral state and state-dependent cognitive processes. *Brain Res. Brain Res. Rev.* **42**, 33–84 (2003).
2. Aston-Jones, G. & Cohen, J. D. An integrative theory of locus coeruleus-norepinephrine function: adaptive gain and optimal performance. *Annu. Rev. Neurosci.* **28**, 403–450 (2005).
3. Sara, S. J. The locus coeruleus and noradrenergic modulation of cognition. *Nat. Rev. Neurosci.* **10**, 211–223 (2009).
4. McCormick, D. A., Pape, H. C. & Williamson, A. Actions of norepinephrine in the cerebral cortex and thalamus: implications for function of the central noradrenergic system. *Prog. Brain Res.* **88**, 293–305 (1991).
5. Kirkwood, A., Rozas, C., Kirkwood, J., Perez, F. & Bear, M. F. Modulation of long-term synaptic depression in visual cortex by acetylcholine and norepinephrine. *J. Neurosci.* **19**, 1599–1609 (1999).
6. Salgado, H. *et al.* Layer-specific noradrenergic modulation of inhibition in cortical layer II/III. *Cereb. Cortex* **21**, 212–221 (2011).
7. Ramos, B. P. & Arnsten, A. F. Adrenergic pharmacology and cognition: focus on the prefrontal cortex. *Pharmacol. Ther.* **113**, 523–536 (2007).
8. Kobayashi, M. Differential regulation of synaptic transmission by adrenergic agonists via protein kinase A and protein kinase C in layer V pyramidal neurons of rat cerebral cortex. *Neuroscience* **146**, 1772–1784 (2007).
9. Trevino, M. & Kirkwood, A. Alpha-1 and beta adrenergic receptors facilitate and suppress LTP and LTD in a mutually exclusive manner. *Program No. 335. 16. Neuroscience Meeting Planner. Washington (DC): Society for Neuroscience.*(2008).
10. Huang, S. *et al.* Pull-Push Neuromodulation of LTP and LTD Enables Bidirectional Experience-Induced Synaptic Scaling in Visual Cortex. *Neuron* **73**, 497–510 (2012).
11. Kirkwood, A. & Trevino, M. Neuromodulation of associative plasticity in visual cortex. *FENS Abstr. , vol. 4, 215. 13*(2008).
12. Sjostrom, P. J., Rancz, E. A., Roth, A. & Hausser, M. Dendritic excitability and synaptic plasticity. *Physiol Rev.* **88**, 769–840 (2008).
13. Nelson, S., Toth, L., Sheth, B. & Sur, M. Orientation selectivity of cortical neurons during intracellular blockade of inhibition. *Science* **265**, 774–777 (1994).
14. Yazaki-Sugiyama, Y., Kang, S., Cateau, H., Fukai, T. & Hensch, T. K. Bidirectional plasticity in fast-spiking GABA circuits by visual experience. *Nature* **462**, 218–221 (2009).
15. Dudek, S. M. & Friedlander, M. J. Intracellular blockade of inhibitory synaptic responses in visual cortical layer IV neurons. *J. Neurophysiol.* **75**, 2167–2173 (1996).
16. Goldman-Rakic, P. S., Lidow, M. S. & Gallager, D. W. Overlap of dopaminergic, adrenergic, and serotoninergic receptors and complementarity of their subtypes in primate prefrontal cortex. *J. Neurosci.* **10**, 2125–2138 (1990).
17. Pawlak, V., Wickens, J. R., Kirkwood, A. & Kerr, J. N. Timing is not Everything: Neuromodulation Opens the STDP Gate. *Front Synaptic. Neurosci.* **2**, 146 (2010).
18. Seol, G. H. *et al.* Neuromodulators control the polarity of spike-timing-dependent synaptic plasticity. *Neuron* **55**, 919–929 (2007).
19. Froemke, R. C. & Dan, Y. Spike-timing-dependent synaptic modification induced by natural spike trains. *Nature* **416**, 433–438 (2002).
20. Feldman, D. E. Timing-based LTP and LTD at vertical inputs to layer II/III pyramidal cells in rat barrel cortex. *Neuron* **27**, 45–56 (2000).
21. Zhang, J. C., Lau, P. M. & Bi, G. Q. Gain in sensitivity and loss in temporal contrast of STDP by dopaminergic modulation at hippocampal synapses. *Proc. Natl. Acad. Sci. U. S A* **106**, 13028–13033 (2009).

22. Abbott, L. F. & Nelson, S. B. Synaptic plasticity: taming the beast. *Nat. Neurosci.* **3 Suppl**, 1178–1183 (2000).
23. Trevino, M., Frey, S. & Köhr, G. Alpha-1 Adrenergic Receptors Gate Rapid Orientation-Specific Reduction in Visual Discrimination. *Cereb. Cortex* (2011).
24. Trevino, M., Vivar, C. & Gutierrez, R. Excitation-inhibition balance in the CA3 network--neuronal specificity and activity-dependent plasticity. *Eur. J. Neurosci.* **33**, 1771–1785 (2011).
25. Chiti, Z. & Teschemacher, A. G. Exocytosis of norepinephrine at axon varicosities and neuronal cell bodies in the rat brain. FASEB J. **21**, 2540–2550 (2007).
26. Crick, F. & Mitchison, G. The function of dream sleep. *Nature* **304**, 111–114 (1983).
27. Tononi, G. & Cirelli, C. Sleep function and synaptic homeostasis. *Sleep Med. Rev.* **10**, 49–62 (2006).
28. Diekelmann, S. & Born, J. The memory function of sleep. *Nat. Rev. Neurosci.* **11**, 114–126 (2010).
29. Hu, H. *et al*. Emotion enhances learning via norepinephrine regulation of AMPA-receptor trafficking. *Cell* **131**, 160–173 (2007).

Acknowledgments

We thank the German Federal Ministry of Science and Research (BMBF) for generous support (01DN12062). We thank Dr. R. Sprengel for scientific advice and J. Ledderose for staining 42 biocytin filled cells. M.T. was supported by a Max Planck Fellowship. We thank P.H. Seeburg for constant support.

Author contributions

M.T. designed the study and planned the experiments. H.S. and M.T. performed experiments and analyzed data. All authors wrote and reviewed the manuscript.

Additional information

Competing financial interests: The authors declare no competing financial interests.

How to cite this article: Salgado, H., Köhr, G. & Treviño, M. Noradrenergic 'Tone' Determines Dichotomous Control of Cortical Spike-Timing-Dependent Plasticity. *Sci. Rep.* **2**, 417; DOI:10.1038/srep00417 (2012).